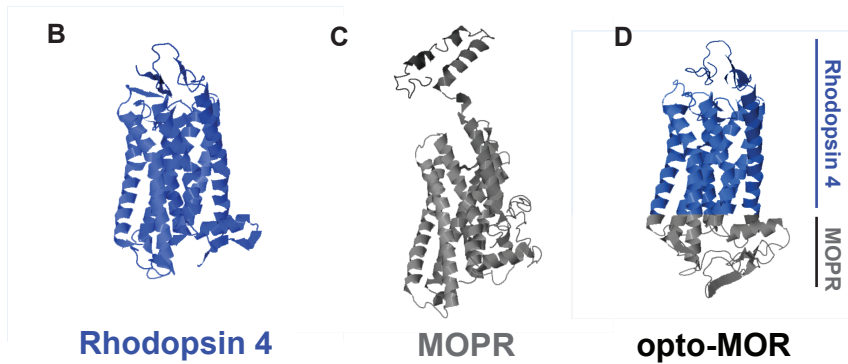
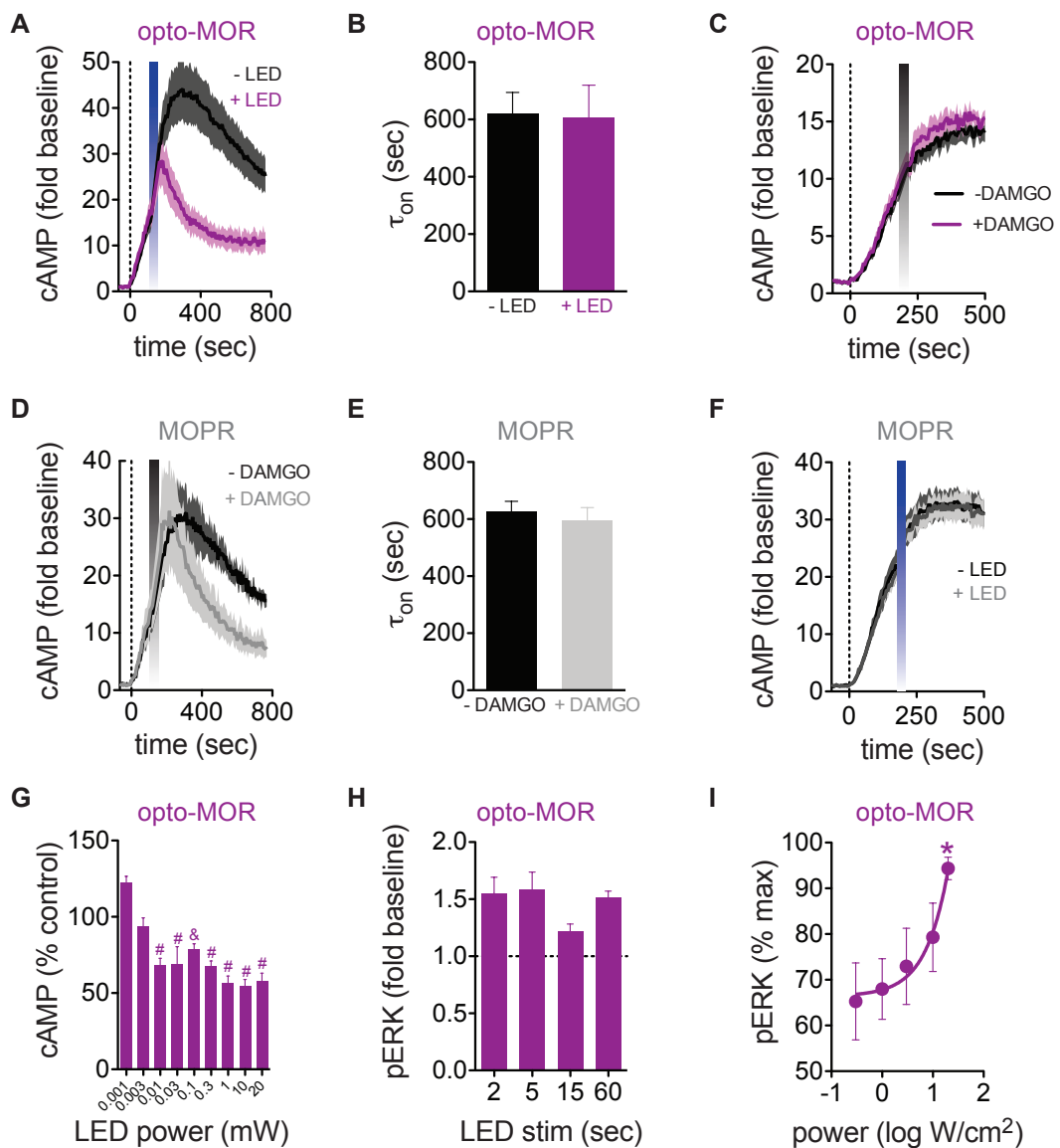


**A**

N-Terminus			
MNGTEG-----PNFYVPSNIT-----GVVRSPFEQPQYYLAEPWQFSML		40	rhod-R04
MDSSTG-----PGNTSDCSDPLAQASCSPAPGSWL-NLSHVDGNQSDPCGLNRTGLGGNDS-LCPQTGSPSMVTAITIM		72	MOR
MNGTEG-----PNFYVPSNIT-----GVVRSPFEQPQYYLAEPWQFSML		40	opto-MOR
<b>TM1</b>	<b>C1</b>	<b>TM2</b>	<b>E1</b> <b>TM3</b>
AAYMFLIIVLGFPINFLTYVQHKLRTPLNYYLLNLAVADLFMVFGGFTTLYTSLHGIVFVFGPTGCNLEGFATLG		120	rhod-R04
ALYSIVCVV-GLFGNFLMYYIVRYTKMKATATNIYIFNLALADALATST-LPFQSVNYLMGTWPFGTILCKIVISIDYIN		150	MOR
AAYMFLIIVLGFPINFLTYVIVRYTKMKATATNIYIFNLALAVADLFMVFGGFTTLYTSLHGIVFVFGPTGCNLEGFATLG		120	opto-MOR
<b>TM3</b>	<b>C2</b>	<b>TM4</b>	<b>E2</b>
GEIGLWSLVLAIERYVWCKPMSNFRFEGEN-HAIMGVAFTWWMALACAAPPLY-GWSRYIP--EGMQCSCGIDYYTLKP		196	rhod-R04
MFTSIFTLCTMSVDYRIVACHPKVAKLDFRTPRNAIKIVNVCNWILSSAIGLPVMFMATTKYRQ--GSID--CTLTFS--HP		224	MOR
GEIGLWSLVLAIERYVWCHPKVAKLDFRTPRNAIMGVAFTWWMALACAAPPLY-GWSRYIP--EGMQCSCGIDYYTLKP		197	opto-MOR
<b>TM5</b>	<b>C3</b>	<b>TM6</b>	
EV--NNESFVIYMFVYHFTIPMIVIFFCYQLVETVKEAAAQDESATTQKAEKVEVTRMVIIMVIFFLICHLPYASVAMY		274	rhod-R04
TW-YWENLLKICVFIFAFIMPLVIITVCGGLMILRLK-SVRMLSGSKEKDRNLRRIITRMVLYVAVFVVCWTPIHIVYII		302	MOR
EV--NNESFVIYMFVYHFTIPMIVIFFCYQLVETVKEAAAQDESATTQKAEKVEVTRMVIIMVIFFLICHLPYASVAMY		274	opto-MOR
<b>E3</b>	<b>TM7</b>	<b>C-Terminus</b>	
IFTHQGSN--FGPIFMTLPFAFFATASIYNPIIYIMN---KQ-FRNCMLTTLCCGKNPLG-----DDEAS-----		334	rhod-R04
KALITIPETTFQTVSWHFICIALQYTNISCLNPVLYAFLDENFKRCREF-----CIPTSSSTIEQQNSTRVRQNTREHPSTANTVDR		382	MOR
IFTHQGSN--FGPIFMTLPFAFFATASIYNPIIYIMN---KQ-FREF-----CIPTSSSTIEQQNSTRVRQNTREHPSTANTVDR		348	opto-MOR
ATASK-----TETSQVAPA		348	rhod-R04
TNHQLENLEAETAPLP-----		398	MOR
TNHQLENLEAETAPLP-----TETSQVAPA		373	opto-MOR



**Figure S1 Related to Figure 1. Design and construction of opto-MOR as a chimeric receptor based on rat rhodopsin 4 and rat MOR. (A)** Sequence alignment of R04 and MOPR generated by COBALT (NCBI; [http://www.ncbi.nlm.nih.gov/tools/cobalt/re\\_cobalt.cgi](http://www.ncbi.nlm.nih.gov/tools/cobalt/re_cobalt.cgi)). The rhodopsin 4 sequence (blue font) and the MOPR sequence (black font) were merged to form a chimera that retained the extracellular and transmembrane aspects of R04 and the intracellular loops of MOPR (shaded gray). The opto-MOR sequence also retains the critical retinal binding site of rhodopsin (shaded blue). Predicted protein structures were generated using the I-TASSER platform and show that rhodopsin 4 (**B**) and MOPR (**C**) combine to form the 7 transmembrane protein, opto-MOR chimera (**D**) that retains critical features for function of each receptor.



**Figure S2, Related to Figure 1: Opto-MOR and MOR share similar cAMP and pERK signaling mechanisms. (A)** Data from Figure 1D expressed as fold baseline. **(B)** Time constants of on rates ( $\tau_{on}$ ) fit from Figure 1D. **(C)** Opto-MOR is not responsive to DAMGO (1  $\mu$ M) application. **(D)** Data from Figure 1E expressed as fold baseline. **(E)** Time constants of on rates ( $\tau_{on}$ ) fit from Figure 1E. **(F)** MOPR is not responsive to light stimulation (15 sec, 1 mW). **(G)** Power response data from opto-MOR (n = 3-10 experiments; @ p < 0.05, # p < 0.001 via One Way ANOVA followed by Dunnett's Multiple Comparison Test to 0.001 mW group). **(H)** Different light pulse lengths produce similar increases in pERK in opto-MOR (n = 3 experiments). **(I)** pERK power response of opto-MOR (n = 6 experiments; \* p < 0.05 via One Way ANOVA followed by Dunnett's Multiple Comparison Test to 0.3 W/cm<sup>2</sup> group). Data are represented as mean  $\pm$  SEM.

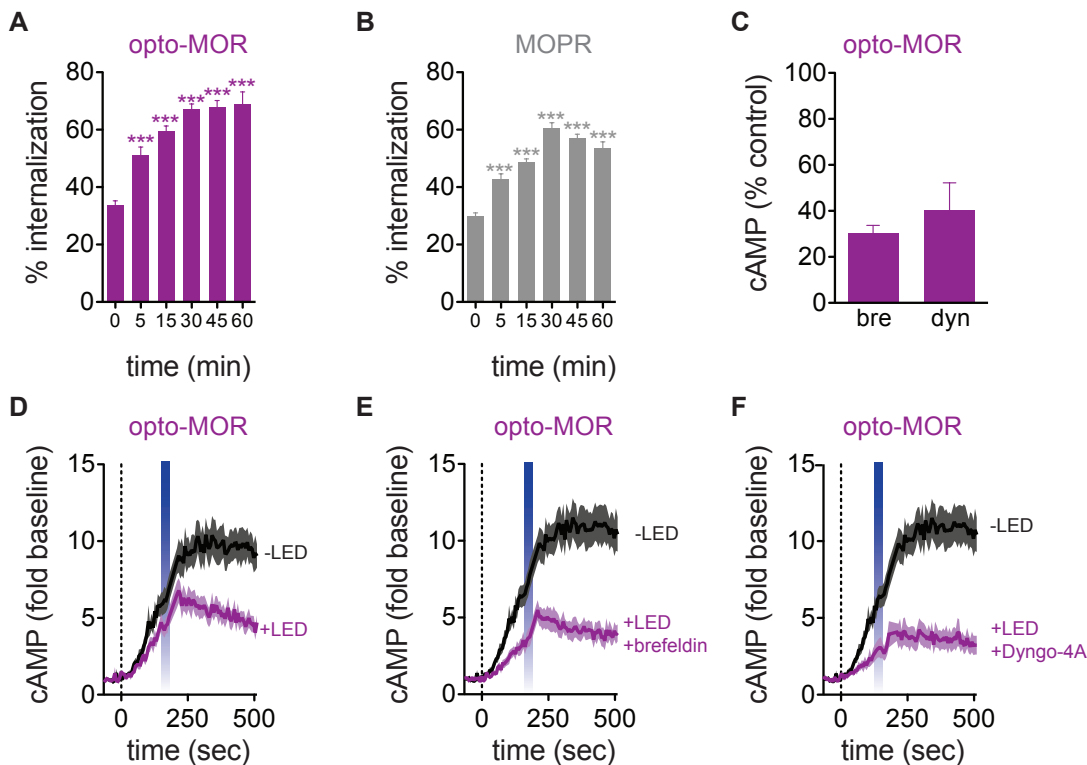


**Figure S3, Related to Figure 2: Opto-MOR and MOPR internalization and recovery from desensitization.** (A) Percent internalization for opto-MOR ( $n = 16-43$  cells over 2 experimental replicates). (B) Percent internalization for MOPR ( $n = 24-38$  cells over 3 experimental replicates). (\*\*\*)  $p < 0.001$  via One Way ANOVA followed by Dunnett's Multiple Comparison Test to 0 time point). (C) Pharmacological treatment of recovery from desensitization; bre = brefeldin A; dyn = Dyngo-4a. (D) Opto-MOR recovery from desensitization following 1 hour prepulse. ( $n = 9-10$  replicates). (E) Opto-MOR inhibition of cAMP in the presence of Brefeldin A ( $5 \mu\text{M}$ ;  $n = 11-12$  replicates). (F) Opto-MOR inhibition of cAMP in the presence of Dyngo-4a ( $30 \mu\text{M}$ ;  $n = 10-11$  replicates). Dashed lines in D-F represent addition of forskolin ( $1 \mu\text{M}$ ). Data are represented as mean  $\pm$  SEM.

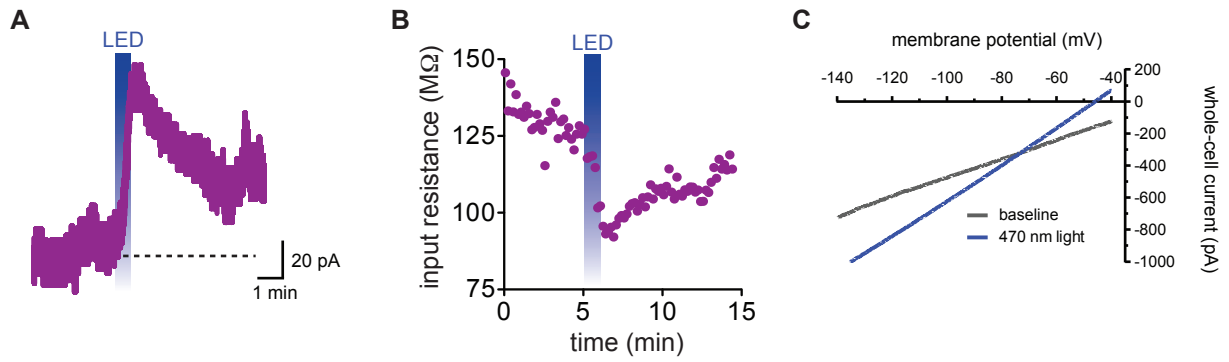


**Figure S4, Related to Figure 4: Opto-MOR activation in GABAergic neurons of the RMTg.** (A) Representative current trace of an opto-MOR<sup>+</sup> neuron in the RMTg in response to 30s stimulation with blue LED light (10 mW/mm<sup>2</sup>), showing a rapid outward current. (B) Plot of the simultaneous decrease in input resistance following LED illumination. (C) Current-voltage plot elicited by a 250 ms ramping voltage stimulus from -40 mV to -140 mV before (black) and after LED illumination (blue). The change in slope is indicative of GIRK channel activation.

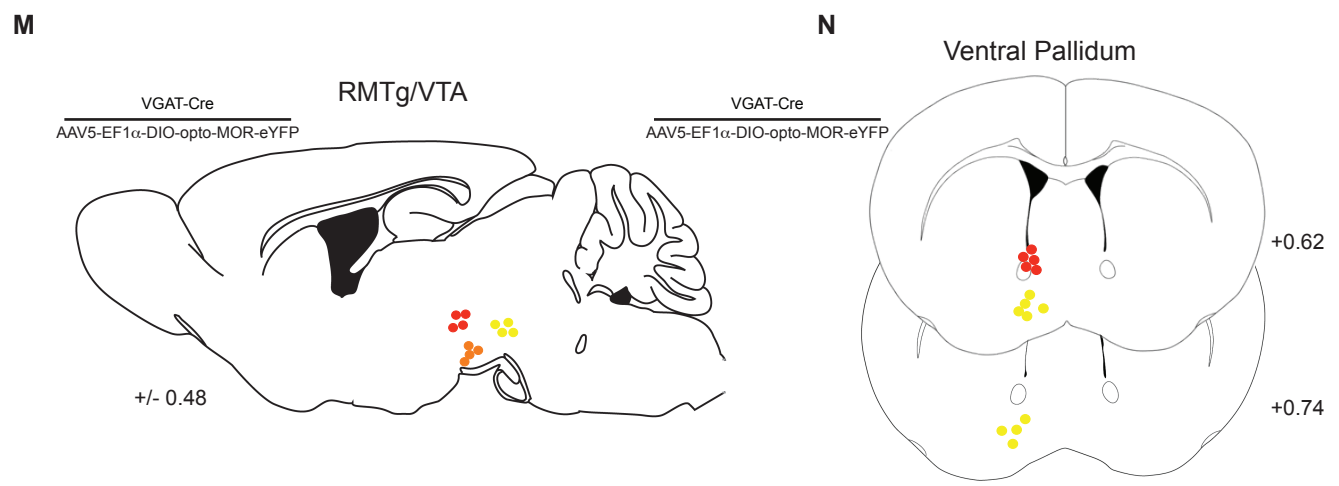
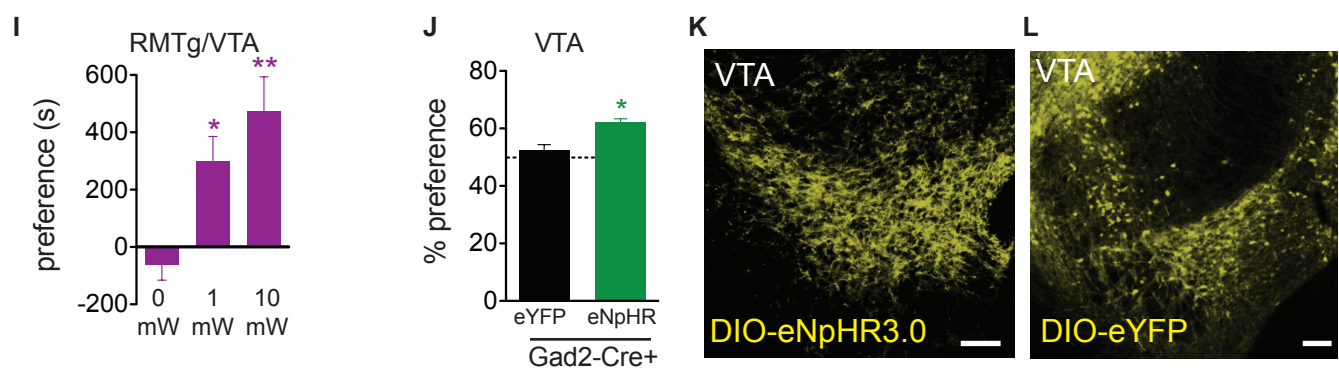
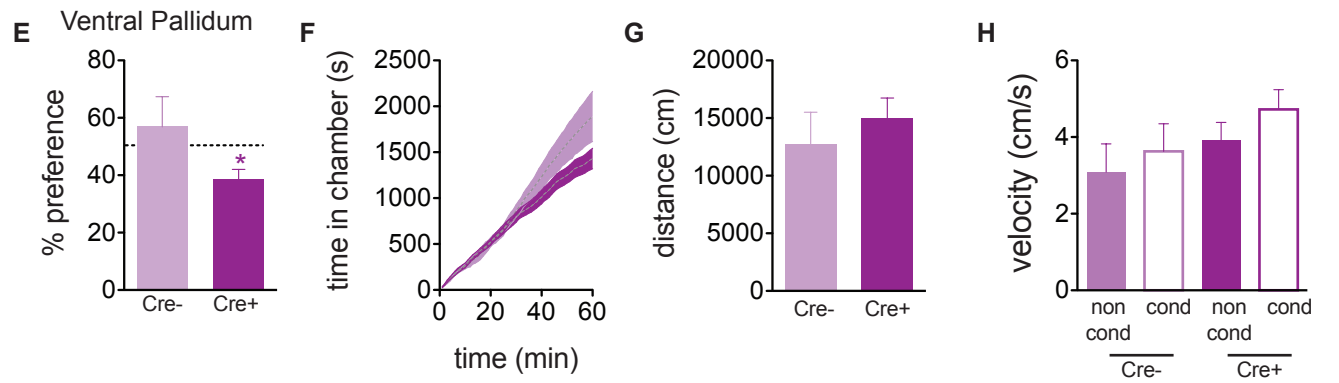
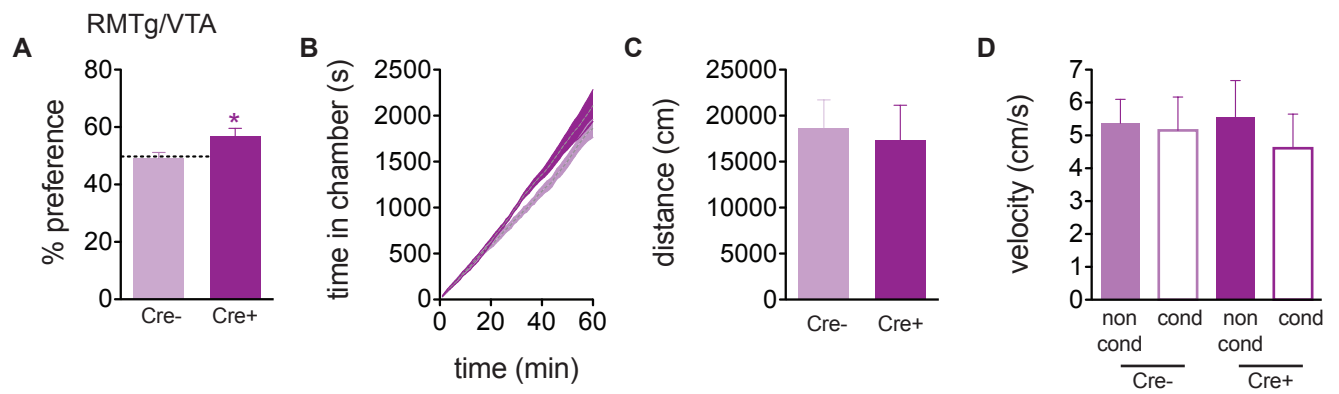


**Figure S5, Related to Figure 6: Photostimulation of vGAT-IRES-Cre<sup>opto-MOR</sup> expressing mice induces selective effects on reward/aversion behavior without affecting general locomotor activity.** vGAT-IRES-Cre<sup>opto-MOR:RMTg</sup> mice (n=8) display significantly increased place preference compared to Cre- littermate controls (n=7) **(A)** developing over the course of the entire session **(B)**. However, locomotor distance travelled **(C)** and velocity during light stimulation **(D)** were unaffected. Similarly, vGAT-IRES-Cre<sup>opto-MOR:VP</sup> mice (n=16) display significantly decreased place preference compared to Cre- littermates (n=5) **(E)** over the course of the session **(F)** in the absence of any changes in locomotor distance **(G)** and velocity **(H)**. **(I)** vGAT-IRES-Cre<sup>opto-MOR:RMTg</sup> mice show increased real time place preference with increasing light power (1 mW (n = 7), 10 mW (n = 7)) compared to no light (0 mW (n = 5)); (\*p < 0.05, \*\*p < 0.01 via One-Way ANOVA followed by Dunnett's multiple comparison test to 0 mW. GABAergic interneurons of the VTA expressing halorhodopsin display similar real time place preference behaviors **(J)** that are comparable to the RMTg-VTA opto-MOR group. **(K-L)** Show expression of DIO-eNpHR3.0 and DIO-eYFP in the VTA (\*p<0.05 via Unpaired t-test). **(M)** Sagittal sections confirming representative slices of viral expression and fiber optic implant placement. Red = fiber optic tip; orange = projections of RMTg from VTA; yellow = injection site and viral expression in RMTg. **(N)** Coronal section confirming representative viral expression and fiber optic implant placement. Red = fiber optic tip; yellow = injection site and viral expression in VP. Data are represented as mean ± SEM.

## Supplemental Experimental Procedures:

### Cell Culture

Cells were cultured in Dulbecco's modified Eagle's media (DMEM), 10% fetal bovine serum, 0.5% Pen/Strep, and 0.5% Amphotericin B. Opto-MOR and rat MOR containing pcDNA3 plasmids were stably transfected into HEK293 cells and maintained under 400 µg/ml geneticin (G418) selection. All *in vitro* studies utilizing opto-MOR contained 10 µM 9-cis retinal (Sigma) in the media to preserve photostable active receptors.

### Preparation of DRG neuronal cultures

DRGs were dissected from 6-7 week old Advillin-Cre mice in HBSS with 10 mM HEPES (HBSS+H) and first digested with 45U papain (Worthington Biochemical) for 20 min at 37°C. Ganglia were washed with HBSS+H and further digested in 1.5 mg/ml collagenase (Sigma) at 37°C for 20 min. Neurons were washed with HBSS and resuspended in Neurobasal media (Gibco) containing 5% FBS (Life Technologies), and supplemented with 1x B27 (Gibco), 2 mM Glutamax (Life Technologies) and 100 U/ml penicillin/streptomycin (Life Technologies). Ganglia were then triturated through a flame-polished Pasteur pipette 6 times, before being filtered through a 40 µm nylon cell strainer (Falcon). Following centrifugation and washing with DRG media, cells were plated onto 12 mm coverslips coated with collagen and poly-D-lysine (both from Sigma). Neurons were grown in a humidified incubator at 37°C in 5% CO<sub>2</sub>. For pERK staining, DRG cultured coverslips were fixed for 15 with 4% paraformaldehyde then rinsed 3x with PBS, permeabilized and blocked in (3% GS, 0.3% Triton X-100) for 20 min @RT. Coverslips were then washed 3x with PBS and incubated in primary antibody (mouse monoclonal pERK (Cell Signaling 9106; 1:500) diluted in PBS (with 3% GS, no Triton) overnight at 4°C. Coverslips were then washed 3x with PBS and secondary antibody (Goat α mouse Alexa Fluor 594; A11032) for 1 hr at RT, then washed 5x in PBS, mounted cell side down in ProLong Gold antifade +DAPI (Life Technologies P36931).

### Slice Physiology

Whole-cell patch-clamp recordings were made using fire-polished glass pipettes with a resistance of 4-7 MΩ filled with (in mM): 120 K<sup>+</sup> gluconate, 5 NaCl, 2 MgCl<sub>2</sub>, 0.1 CaCl<sub>2</sub>, 10 HEPES, 1.1 EGTA, 4 Na<sub>2</sub>ATP, 0.4 Na<sub>2</sub>GTP, 15 phosphocreatine; pH adjusted to 7.3 with KOH, 291 mOsm. The liquid junction potential was calculated to be 16.2 mV and was not corrected. Slices were transferred to the recording chamber in the dark and perfused (~2 mL/min) with oxygenated aCSF containing (in mM): 124 NaCl, 2.5 KCl, 1.2 NaH<sub>2</sub>PO<sub>4</sub>, 24 NaHCO<sub>3</sub>, 5 HEPES, 12.5 glucose, 2 CaCl<sub>2</sub>, 1 MgCl<sub>2</sub>; pH=7.3, 300-325 mOsm. GABAergic neurons in the PAG were visualized through a 40x objective using IR-DIC microscopy on an Olympus BX51 microscope, and YFP<sup>+</sup> neurons were identified using epifluorescent illumination.

Recordings were made with Patchmaster software controlling a HEKA EPC10 amplifier. Following gigaseal formation and stable whole-cell access, currents elicited by stimulation of opto-MOR and MOPR were isolated by blocking AMPA/KARs (10 µM NBQX, Abcam), NMDARs (50 µM D-APV, Abcam), GABA<sub>A</sub>Rs (100 mM picrotoxin, Abcam), and GABA<sub>B</sub>Rs (50 µM saclofen, Abcam). Neurons were voltage clamped at -60 mV and whole-cell currents were recorded using a gap-free protocol with regular test-pulses to monitor input resistance (-10 mV every 10 sec, 5 kHz sampling rate). Only cells with a stable R<sub>s</sub> < 35 MΩ were included in our analysis. For current-clamp recordings, neurons were held at ~-65 mV and data was sampled at 20 kHz. Input resistance and excitability was determined with a series of 1 second current steps from

-20 pA to +100 pA in 10 pA increments. Ramp currents were elicited following a prepulse to -20 mV for 500 ms, then neurons were hyperpolarized to -120 mV over a 250 ms interval. Light stimulation was delivered through the objective with a 470 nm LED coupled to the back fluorescent port of the microscope, and light intensity was 10 mW/mm<sup>2</sup> at the surface of the slice. GIRK currents were blocked by adding 1 mM BaCl<sub>2</sub> to the antagonist cocktail while endogenous MOPRs were stimulated with 1 μM DAMGO (Tocris).

### **Statistical Methodology and Data analysis**

All data are expressed as mean ± SEM. Statistical significance was taken as \*p < 0.05, \*\*p < 0.01, \*\*\*p < 0.001, as determined by the Student's t-test (paired and unpaired): One-Way Analysis of Variance (ANOVA) or One-Way Repeated Measures ANOVA, followed by Dunnett's or Bonferroni *post hoc* tests as appropriate. Statistical analyses were performed in GraphPad Prism 6.0.